Robust Multi-stage Power Grid Operations with Energy Storage

Yihan Zou, Xiaojun Lin, Dionysios Aliprantis
School of Electrical & Computer Engineering,
Purdue University, West Lafayette, IN, USA
Email: {zou59, linx, dionysios}@purdue.edu

Minghua Chen
Department of Information Engineering,
The Chinese University of Hong Kong
Email: minghua@ie.cuhk.edu.hk

***Abstract*—The uncertainty and variability of renewable generation pose significant challenges to reliable power-grid operations. This paper designs robust online strategies for jointly operating energy storage units and fossil-fuel generators to achieve provably reliable grid operations at all times under high renewable uncertainty, without the need of renewable curtailment. In particular, we jointly consider two power system operations, namely day-ahead reliability assessment commitment (RAC) and real-time dispatch. We first extend the concept of "safe-dispatch sets" to our setting. While finding such safe-dispatch sets and checking their non-emptiness provide crucial answers to both RAC and real-time dispatch, their computation incurs high complexity in general. To develop computationally-efficient solutions, we first study a single-bus case with one generator-storage pair, where we derive necessary conditions and sufficient conditions for the safe-dispatch sets. Our results reveal fundamental trade-offs between storage capacity and generator ramp-up/-down limits to ensure grid reliability. Then, for the more general multi-bus scenario, we split the net-demand among virtual generator-storage pairs (VGSPs) and apply our single-bus decision strategy to each VGSP. Simulation results on an IEEE 30-bus system show that, compared with state-of-art solutions, our scheme requires significantly less storage to ensure reliable grid operation without any renewable curtailment.**

I. Introduction

While renewable energy is considered crucial for a sustainable energy future, its uncertainty and variability pose significant challenges to the reliable operations of power systems [1]. In electricity grids, the demand and supply must be balanced at all time, subject to various physical limits on generation and transmission. The higher uncertainty and variability of renewable resources makes it challenging to determine how many generation resources need to be committed ahead of time, and how to dispatch them in real time, to meet the demand. Energy storage can be a key resource to improve grid reliability in this situation because it can shift demand and supply in time [2]. However, storage also has it own operation limits, and hence adding storage into the resource pool also introduces new questions on how to operate both generators and storage units to maintain reliable grid operations at all times.

In this paper, we study these questions at the Independent System Operator (ISO) level. An ISO is responsible for maintaining reliable grid operations in a large geographic area [3]. An ISO operates the wholesale electricity market, which usually includes a day-ahead market and a real-time market [4] [5]. The day-ahead market is a forward market that allows market participants to commit the amount of energy to buy or sell in each hour of the following day. A key part of the day-ahead operation, including both market clearance and the later RAC[1] (Reliability Assessment and Commitment) stage, is to set aside enough resources ahead of time to meet the demand in the next day. Then, when the operating day comes, the real-time market dispatches resources every 5 minutes to match the supply to any demand deviation from day-ahead predictions. Thus, in this paper we aim to provide solutions, both for RAC and real-time dispatch, to the problem of managing generators and storage to provably ensure reliable grid operations under high renewable uncertainty.

One key challenge to this problem is the multi-stage nature of the operation decisions. In practice, the availability of uncertain renewable supply is revealed sequentially over time. The ISO only knows the information up to the present time, yet decisions must be made despite future uncertainty. This *causality* (also known as *non-anticipativity*) requirement cannot be violated during the decision making process. However, a large body of existing literature uses a two-stage assumption, which does not respect this multi-stage nature. Under such a two-stage assumption, one assumes that there is a second stage where uncertainty is completely revealed [6] [7]. In practice, such a second stage with perfect information does not exist. As a result, such a two-stage approach can significantly underestimate the resource requirement for reliability [8] [9] [10].

There is a limited body of work that directly deals with this multi-stage problem, with or without energy storage. In [8], the authors use affine policies to solve this multi-stage decision problem using only generators. This approach is further extended in [9] to work with storage units. However, a common weakness in [8] and [9] is that such an affine policy treats resources with different capabilities in the same manner, which tends to be overly conservative (see further discussion in Section III-C). Partly due to this reason, [9] must assume renewable curtailment so that the demand-supply balance can always be met despite this inefficiency. In our prior work [10], we show that by pairing generators of different ramping speeds, one can support reliable grid operations at a higher level of uncertainty than what affine policies allow. On the other hand, [10] does not deal with energy storage. As the reader will see in Section III, the operation characteristics

[1]Note that RAC can also be performed during real-time operation when future operating conditions change significantly, for which our proposed methodology can also be applied. We mainly focus on day-ahead RAC because a "late" RAC usually needs to commit more-expensive fast generation.

of energy storage are very different from generators. Thus, the following open question remains: if one does not allow renewable curtailment, how can generators and storage be used together in a complementary manner to maintain reliable multi-stage grid operations under high renewable uncertainty?

To address this open question, in this paper we develop new efficient methods to manage generators and storage units in both RAC and real-time dispatch that can provably ensure reliable grid operations at all times without the need of renewable curtailment. Specifically, in Section II we extend the notion of "safe dispatch sets" of [10], which contain decision points at the current time that can guarantee grid safety[2] at all times in the future. By definition, verifying the non-emptiness of the safe dispatch set at day-ahead RAC ensures grid safety for the entire next day, and real-time dispatch can simply pick dispatch decisions from the safe dispatch set at each time (see [10] and Section II-D). However, the computation of such safe dispatch sets incurs high complexity in general. To develop computationally efficient solutions, in Section III we first focus on a single-bus system with one generator and one storage unit, and study how their different operation characteristics complement each other. We derive both necessary conditions and sufficient conditions for grid safety, which are tight under certain circumstances. Thus, our results reveal fundamental trade-offs between storage capacity and generator ramp-up/-down limits to ensure reliability. Further, our key technical contribution is to identify a "flat-top/flat-bottom" property (see Section III-B), which breaks down the dependency across stages, and leads to easy-to-verify sufficient conditions for the safe dispatch sets. Then, for the more general multi-bus scenario in Section IV, we optimize affine demand splitting to "virtual generator-storage pairs" (VGSPs) to obtain a computationally-efficient characterization of a provable subset of the true safe dispatch set. Numerical results in Section V demonstrate that, compared to [9], our approach requires significantly less storage to ensure reliable grid operations when renewable curtailment is not allowed, especially when the decision horizon is large. Even if curtailment is allowed as in [9], our solution tends to utilize a higher level of renewable supply.

II. System Model

We now present the system model for reliable grid operations with energy storage, when renewable curtailment is not allowed. There is a set of N_b buses $\mathcal{B} = \{1, 2, \ldots, N_b\}$ that are inter-connected by a set of N_l transmission lines $\mathcal{L} = \{1, 2, \ldots, N_l\}$. There could be multiple generators, renewable sources, storage units, and/or loads on each bus.

We adopt a discrete-time model for decision making. During real-time operation, at the beginning of each time slot, the ISO needs to make a decision that is going to last for the entire time slot. Assume that the operation horizon is divided into T time slots. To model the day-ahead decision, we assume that a set of generators and storage are already committed, our goal is to check if this set of resources are sufficient for reliable grid operations for the entire horizon. Note that this is part of the RAC decision. (The other part is to decide which units to commit.) In the following paragraphs, we introduce the notations and characteristics of various system components.

A. Demand Side

On each bus b, we take renewable supply as negative load, and define the uncertain net-demand $D_b(t)$ at bus b at time t as the load minus the renewable supply. Let $D_b(t_1 : t_2)$ denote the net-demand sequence at bus b from time t_1 to t_2. Let $D(t_1, t_2)$ denote the collection of net-demand sequences $D_b(t_1, t_2)$ on all buses. Note that here we implicitly assume that renewable is not curtailed. There are two motivations that justify this assumption. First, if the renewable supply is "behind-the-meter," e.g., as in the case of rooftop solar, it is not under the control of the ISO and thus cannot be easily curtailed. Second, since renewable supply often has lower daily operation cost than fossil-fuel generation, it is desirable to utilize renewable energy as much as possible. Thus, even though curtailing renewable energy may help to ensure reliable grid operation in some cases, it does so at the cost of efficiency and economy. Hence, it would still be interesting, and practically useful, to study how to ensure reliable grid operations without the need of renewable curtailment.

Next, we model the uncertainty of net-demand. We define the uncertainty set $\mathcal{D}$ as the set of all net-demand sequences $D(1 : T)$ for which we wish to ensure reliable grid operations. Throughout this paper, we are interested in an uncertainty set of the following form:

$$D_b^{\min}(t) \le D_b(t) \le D_b^{\max}(t), \text{ for all } t, \tag{1}$$

$$|D_b(t_1) - D_b(t_2)| \le \Delta_b |t_1 - t_2|, \text{ for all } t_1, t_2, \tag{2}$$

where the parameters $D_b^{\min}(t)$ and $D_b^{\max}(t)$ represent the lower and upper bounds, respectively, for the net-demand on bus b at time t. $\Delta_b \ge 0$ denotes the maximum rate of change in net-demand on bus b. The constraint in (2) models that renewable supply does not change arbitrarily fast. These parameters can be obtained from historical data and day-ahead prediction [11]. Notice that, although the uncertainty set $\mathcal{D}$ contains net-demand sequences for the entire time horizon, at time t the ISO only sees the realization of net-demand *up to* t. Unlike a two-stage model where the entire net-demand is revealed at a second stage [6] [7], here the future values of $D(t+1 : T)$ are still unknown to the ISO. Nonetheless, the constraint in (2) can be used to refine the future uncertainty based on the revealed history, which can be viewed as some form of "near-term prediction." Specifically, given $D(1 : t)$, the set of possible future net-demand trajectories $D(t_1, t_2), t_1, t_2 > t$, tends to be smaller, which we denote by

$$\mathcal{D}_{[t_1:t_2]|D(1:t)} = \big\{ D(t_1 : t_2) | \text{ there exist } D'(1 : T) \in \mathcal{D}, \text{ such that } D'(1 : t) = D(1 : t), \text{ and } D'(t_1 : t_2) = D(t_1 : t_2) \big\}.$$

[2] In this paper, we use the term "safety" and "reliability" interchangeably, which both mean that demand and supply have to be balanced at all time subject to physical limits (also related to "resource adequacy").

B. Supply Side

Next, we formulate the mathematical models for generators and storage units, which the ISO dispatches to balance the uncertain net-demand at all time.

1) Generators: We restrict the term "generators" to dispatchable fossil-fuel generation units. (Recall that renewable generation is treated as negative load.) Let $\mathcal{G} = \{1, 2, ..., N_g\}$ be the set of generators in the system, and $P_g(t)$ be the power level of generator $g \in \mathcal{G}$ at time t. Each generator has to operate within its capacity range, i.e.,

$$P_g^{\min} \leq P_g(t) \leq P_g^{\max}, \forall g \in \mathcal{G}, t = 1, 2, \ldots, T, \quad (3)$$

where $P_g^{\min}$ and $P_g^{\max}$ denote the lower and upper power limits, respectively, of generator g. Since storage alone will not be able to sustain extended periods of demand-supply imbalance, we assume that $P_g^{\max} \geq D^{\max}(t)$ and $P_g^{\min} \leq D^{\min}(t)$ for all time t. Further, the generator dispatch decisions have to satisfy the following ramping constraint:

$$-R_g \leq P_g(t+1) - P_g(t) \leq R_g, t = 1, 2, \ldots, T-1, \quad (4)$$

where R_g is the ramping speed of generator g. We use $\mathcal{G}_b \subseteq \mathcal{G}$ to denote the set of generators at bus $b \in \mathcal{B}$.

2) Storage units: Let $\mathcal{S} = \{1, 2, ..., N_s\}$ be the set of storage units (e.g., battery and pumped hydro) in the system, and each storage unit $s \in \mathcal{S}$ has a finite capacity $Q_s^{\max}$. We use $Q_s(t)$ to denote the energy storage level (also known as state of charge) of storage s at the end of time-slot t, and $Q_s(0)$ is the initial storage level of unit s. Without loss of generality, we assume that the minimum storage level for each unit is zero. Thus, the storage levels of all units at all time need to satisfy the following capacity constraints:

$$0 \leq Q_s(t) \leq Q_s^{\max}, \forall s \in \mathcal{S}, t = 0, 1, ..., T. \quad (5)$$

One key difference between energy storage units and generators is that the charging/discharging actions are coupled across time. The power provided by storage unit s during time-slot t can be expressed as follows:

$$\Phi_s(t) = Q_s(t-1) - Q_s(t), t = 1, 2, ..., T, \quad (6)$$

where positive (or negative) signs of $\Phi(t)$ correspond to the storage providing (or absorbing) energy. Note that here we have assumed that charging/discharging has no efficiency loss. We will discuss briefly at the end of Section III-B how to generalize our analysis to the case with efficiency loss. Further, for ease of exposition, we have assumed that each slot is of unit length. Thus, the units of Q and Φ are kWh and kWh/slot, respectively. Finally, each storage unit s may also have a power limit $\overline{\Phi}_s$ such that $|\Phi(t)| \leq \overline{\Phi}_s$ for all time t. Let $\mathcal{S}_b$ denote the set of storage units on bus b.

C. Demand-supply Balance & Transmission Constraints

In this work, we assume a DC power flow model [12] and ignore the transmission loss in the system. For reliable grid operations, the total net-power provided by generators and storage units must be equal to the total net-demand at all time, i.e.,

$$\sum_{g \in \mathcal{G}} P_g(t) + \sum_{s \in \mathcal{S}} \Phi_s(t) = \sum_{b \in \mathcal{B}} D_b(t), t = 1, 2, \ldots, T. \quad (7)$$

Further, the transmission-line limits must be obeyed at all time. The DC model formulates the transmission-line constraints using a shift-factor matrix $S = [S_{l,b}]$, each element of which characterizes the contribution from bus b to the power-flow on line l. Thus, the power flow going through line l at time t cannot exceed a value TL_l, which can be written as

$$\left| \sum_{b=1}^{N_b} S_{l,b} \Big(D_b(t) - \sum_{g \in \mathcal{G}_b} P_g(t) - \sum_{s \in \mathcal{S}_b} \Phi(t) \Big) \right| \leq \mathrm{TL}_l, \quad \forall t = 1, 2, \ldots, T; \forall l \in \mathcal{L}. \quad (8)$$

D. Objectives of Online Multi-stage Decisions

We first introduce the following definitions.

Definition 1 (Causality)**.** Given an uncertainty set $\mathcal{D}$, a real-time dispatch algorithm $\pi(\mathcal{D})$ is *causal* if, for every time t, the algorithm only uses $D(1:t)$ in producing the dispatch decision $\mathbf{P}^{\pi(\mathcal{D})}(t) = \Big[\big(P_g^{\pi(\mathcal{D})}(t), Q_s^{\pi(\mathcal{D})}(t) \big) | g \in \mathcal{G}, s \in \mathcal{S} \Big]$.

Definition 2 (Robustness)**.** A causal real-time dispatch algorithm $\pi(\mathcal{D})$ is *robust* if and only if, for all net-demand sequence $D(1:T) \in \mathcal{D}$ and at all time t, the dispatch decision $\mathbf{P}^{\pi(\mathcal{D})}(t)$ produced by algorithm $\pi(\mathcal{D})$ satisfies all physical constraints (3)-(8). Further, a causal real-time dispatch algorithm π is *robust given* $D(1:t)$ and $\mathbf{P}(t)$ if and only if, for any possible future net-demand sequence $D(t+1:T) \in \mathcal{D}_{[t+1:T]|D(1:t)}$, the dispatch output $\mathbf{P}^{\pi}(t_1)$ produced by π will satisfy all constraints (3)-(8), for all $t_1 > t$.

The objectives of this work are the following: (i) At RAC, given the uncertainty set $\mathcal{D}$, determine whether there exists a causal and robust real-time dispatch algorithm $\pi(\mathcal{D})$; (ii) At each time t, find the real-time dispatch algorithm $\pi(\mathcal{D})$ to dispatch the generators and storage units based on $D(1:t)$ to meet all physical constraints.

Note that the causality requirement differentiates our online multi-stage decisions from two-stage formulations in the literature. (Readers may refer to [8] and [10] for the limitation of two-stage formulations.) In [10], the authors introduce the notion of safe-dispatch sets, which we extend to our setting. Let $\mathbf{P}(t) = [P_g(t), g \in \mathcal{G}]$ and $\mathbf{Q}(t) = [Q_s(t), s \in \mathcal{S}]$. Note that $\mathbf{Q}(t-1)$ corresponds to the storage levels both at the end of time-slot $t-1$ and at the beginning of time-slot t.

Definition 3 (Safe Dispatch Set)**.** Given past demand sequence $D(1:t)$, the safe dispatch set $\mathcal{F}\big(D(1:t)\big)$ is defined as

$\mathcal{F}\big(D(1:t)\big) = \big\{ [\mathbf{P}(t), \mathbf{Q}(t-1)] \big|$ starting from $\mathbf{P}(t)$ and $\mathbf{Q}(t-1)$, there exists a causal algorithm π that both can balance the demand $D(t)$ subject to the condition (3), (5)-(8), and is robust given $D(1:t) \big\}$. (9)

As argued in [10], once the safe dispatch sets are known, both the RAC and real-time decisions are straight-forward. At RAC, one simply checks whether the safe dispatch set without any revealed net-demand $\mathcal{F}(\emptyset)$ is non-empty. Note that by definition, $\mathcal{F}(\emptyset) \neq \emptyset$ at day-ahead RAC also implies that $\mathcal{F}(D(1:t))$ will be non-empty at all time t during real-time operation. At real-time dispatch at time t, the causal algorithm π can simply pick any $\mathbf{P}(t)$ such that $[\mathbf{P}(t), \mathbf{Q}(t-1)] \in \mathcal{F}(D(1:t))$ that can be reached from $\mathbf{P}(t-1)$, which implies that all physical constraints can be met in the future. Further, such decisions are known to be "maximally-robust," i.e., if these decisions cannot meet all physical constraints, no other algorithms can do under the same uncertainty set $\mathcal{D}$. [10] demonstrates that the true safe-dispatch sets can be calculated via backward induction. However, such a backward induction incurs exponential complexity in the problem size. Thus, our goal in this paper is to develop computationally-efficient methods to characterize the safe-dispatch sets.

III. Single bus w/ one Generator-storage pair

Towards this end, we first focus on a simpler scenario with one bus, one generator g, and one energy storage unit s. For simplicity, we will drop the subscript b for the net-demand because the net-demand $D(t)$ becomes a scalar. Although, we still retain the subscripts g and s to differentiate generator g from storage unit s. Note that in this scenario the safe-dispatch set becomes a set of vectors $(P_g(t), Q_s(t-1))$. This scenario can be compared to the scenario of one fast generator plus one slow generator in [10]. However, the safe-dispatch set for that scenario in [10] only contains the power level of the slow generator, and thus becomes one dimensional. In contrast, our safe-dispatch set is two dimensional and thus much harder to characterize. In the rest of this section, we fix t and $D(1:t)$. We will proceed by proposing the necessary conditions that the generator-storage pair needs to satisfy for reliability. Then, we continue to derive the sufficient conditions. Furthermore, we show that the sufficient conditions are tight under certain circumstances.

A. Necessary Conditions for $(P_g(t), Q_s(t-1)) \in \mathcal{F}(D(1:t))$

We first derive necessary conditions based on the capacity limit $Q_s^{\max}$ of the storage. Suppose that the generator is operated at $P_g(t)$ at time t. Due to the ramp limit R_g of the generator, its future power level at $t' \geq t$ is bounded by $\underline{P}_g^{\text{eff}}(t') \leq P_g(t') \leq \overline{P}_g^{\text{eff}}(t')$, where

$$\overline{P}_g^{\text{eff}}(t') = \min\{P_g(t) + (t'-t)R_g, P_g^{\max}\}, \tag{10}$$

$$\underline{P}_g^{\text{eff}}(t') = \max\{P_g(t) - (t'-t)R_g, P_g^{\min}\}. \tag{11}$$

Thus, to balance demand at t', we must have

$$\overline{P}_g^{\text{eff}}(t') + \Phi_s(t') \geq \max_{D(t') \in \mathcal{D}_{t'|D(1:t)}} \{D(t')\}, \tag{12}$$

$$\underline{P}_g^{\text{eff}}(t') + \Phi_s(t') \leq \min_{D(t') \in \mathcal{D}_{t'|D(1:t)}} \{D(t')\}. \tag{13}$$

Hence, the conditions (12) and (13) implies that: for $\forall t' \geq t$,

$$P_g(t) + (t'-t)R + Q(t'-1) - Q(t') \geq \max_{D(t') \in \mathcal{D}_{t'|D(1:t)}} \{D(t')\}, \tag{14}$$

$$P_g(t) - (t'-t)R + Q(t'-1) - Q(t') \leq \min_{D(t') \in \mathcal{D}_{t'|D(1:t)}} \{D(t')\}. \tag{15}$$

Replacing t' by τ, and (14) and (15) from t to t', we obtain the following necessary conditions:

$$\sum_{\tau=t}^{t'} \overline{P}_g^{\text{eff}}(\tau) + Q_s(t-1) - Q_s(t') \geq \sum_{\tau=t}^{t'} \max_{D(\tau) \in \mathcal{D}_{\tau|D(1:t)}} \{D(\tau)\}. \tag{16}$$

$$\sum_{\tau=t}^{t'} \underline{P}_g^{\text{eff}}(\tau) + Q(t-1) - Q(t') \leq \sum_{\tau=t}^{t'} \min_{D(\tau) \in \mathcal{D}_{\tau|D(1:t)}} \{D(\tau)\}. \tag{17}$$

As $Q(t') \in [0, Q^{\max}]$, from (16) we must have, for $\forall t' \geq t$,

$$Q_s(t-1) \geq -\sum_{\tau=t}^{t'} [P_g(t) + (\tau-t)R_g] + \sum_{\tau=t}^{t'} \max_{D(\tau) \in \mathcal{D}_{\tau|D(1:t)}} \{D(\tau)\}. \tag{18}$$

This condition is shown in Fig. 1a, where $D(t)$ grows at the fastest rate Δ to reach net-demand upper bound $D^{\max}(t')$, and $P_g(t)$ also grows at the fastest rate to meet demand. The area between these two lines gives a lower bound on the storage level $Q_s(t-1)$. Note that (18) for each t' is a linear constraint in $(P_g(t), Q_s(t-1))$ (see yellow dotted lines in Fig. 1b). Intersection of (18) over all t' thus gives a convex constraint, which is shown by the lower blue solid curve in Fig. 1b. Every point on the blue solid curve represents an operation point where the storage has just enough energy to support the fastest increasing demand. Similarly, from (15) we must have:

$$Q_s(t-1) \leq -\sum_{\tau=t}^{t'} [P_g(t) - (\tau-t)R_g] + \sum_{\tau=t}^{t'} \min_{D(\tau) \in \mathcal{D}_{\tau|D(1:t)}} \{D(\tau)\} + Q^{\max}. \tag{19}$$

Intersection of (19) over all $t' \geq t$ gives the upper red solid curve in Fig. 1b. (18) and (19) combined thus produces a convex outer bound of the safe-dispatch set (see Fig.1b), which we refer to as the *"leaf-region"* at time t given $D(t)$. Further, we can rearrange (18) and (19) to get, $\forall t_1, t_2 \geq t$,

$$\xi_{t_1}^{\min}(D(1:t), Q_s(t-1)) \leq P_g(t) \leq \xi_{t_2}^{\max}(D(1:t), Q_s(t-1)),$$

where

$$\xi_{t_1}^{\min}(D(1:t), Q_s(t-1)) = \frac{1}{t_1 - t + 1}\Big(-\sum_{\tau=t}^{t_1} (\tau-t)R_g - Q_s(t-1) + \sum_{\tau=t}^{t_1} \max_{D(\tau) \in \mathcal{D}_{\tau|D(1:t)}} \{D(\tau)\}\Big), \tag{20}$$

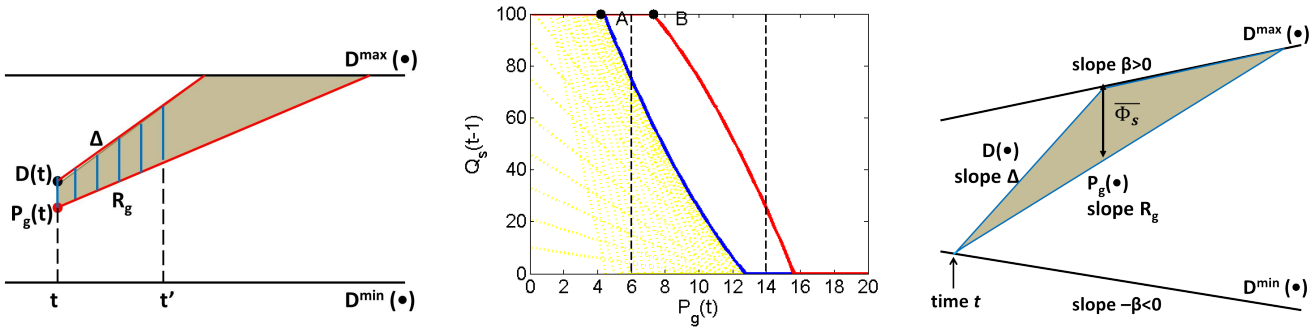

(a) (b) (c)

Fig. 1. (a) If the generator operates at $P_g(t)$, the storage unit needs to supply at least the energy represented by the shaded area. (b) An outer bound of the safe-dispatch set given by the intersection of constraints (18) and (19). (Each yellow line corresponds to (18) for some $t' \geq t$.) (c) An illustration of the storage size needed for meeting the fastest change of demand.

$$\xi^{\max}_{t_2}(D(1:t), Q_s(t-1)) = \frac{1}{t_2 - t + 1}\Big(\sum_{\tau=t}^{t_2}(\tau - t)R_g - Q_s(t-1) + Q^{\max} + \sum_{\tau=t}^{t_2} \min_{D(\tau)\in\mathcal{D}_{\tau|D(1:t)}} \{D(\tau)\}\Big). \quad (21)$$

For example, the points A and B in Fig. 1b correspond to $\min_{t_2\geq t} \xi^{\max}_{t_2}(D(1:t), Q^{\max}_s)$ and $\max_{t_1\geq t} \xi^{\min}_{t_1}(D(1:t), Q^{\max}_s)$, respectively. Thus, a necessary condition for $\mathcal{F}(D(1:t)) \neq \emptyset$ is that there must exist some $Q(t-1) \in [0, Q^{\max}_s]$ such that

$$\max_{t_1\geq t} \xi^{\min}_{t_1}(D(1:t), Q(t-1)) \leq \min_{t_2\geq t} \xi^{\max}_{t_2}(D(1:t), Q(t-1)).$$

Using similar techniques, we can obtain another set of necessary conditions based on the power limit $\overline{\Phi}_s$ of the storage. Specifically, using $|\Phi(t')| \leq \overline{\Phi}_s$ in (12) and (13), we get, for all $t_1, t_2 \geq t$,

$$P_g(t) + (t_1 - t)R_g + \overline{\Phi}_s \geq \max_{D(t_1)\in\mathcal{D}_{t_1|D(1:t)}} \{D(t_1)\}, \quad (22)$$

$$P_g(t) - (t_2 - t)R_g - \overline{\Phi}_s \leq \min_{D(t_2)\in\mathcal{D}_{t_2|D(1:t)}} \{D(t_2)\}. \quad (23)$$

Thus, we have

$$\max_{t_1\geq t} \gamma^{\min}_{t_1}(D(1:t)) \leq P_g(t) \leq \min_{t_2\geq t} \gamma^{\max}_{t_2}(D(1:t)),$$

where

$$\gamma^{\min}_{t_1}(D(1:t)) = \max_{D(t_1)\in\mathcal{D}_{t_1|D(1:t)}} \{D(t_1)\} - (t_1 - t)R_g - \overline{\Phi}_s,$$

$$\gamma^{\max}_{t_2}(D(1:t)) = \min_{D(t_2)\in\mathcal{D}_{t_2|D(1:t)}} \{D(t_2)\} + (t_2 - t)R_g + \overline{\Phi}_s.$$

A necessary condition for $\mathcal{F}(D(1:t)) \neq \emptyset$ is then $\max_{t_1\geq t} \gamma^{\min}_{t_1}(D(1:t)) \leq \min_{t_2\geq t} \gamma^{\max}_{t_2}(D(1:t))$. Note that this condition further reduces the safe-dispatch set (see the vertical dashed lines in Fig. 1b). We will thus refer to the part of the leaf-region between these two vertical dashed lines as the *"cropped leaf-region"* at time t given $D(t)$.

Based on these necessary conditions, we can obtain useful necessary conditions on the storage size needed for reliability. Next, we focus on the case where the net-demand upper/lower bounds are linear and symmetric. More precisely, the upper bound $D^{\max}(\cdot)$ and lower bound $D^{\min}(\cdot)$ are straight lines with slope $\beta \geq 0$ and $-\beta \leq 0$, respectively (see Fig.1c). The following lemma thus gives a lower bound on the required storage size when the time-horizon is long.

Lemma 4 (Minimum Storage Size)**.** *Suppose that the demand upper/lower bounds are linear and symmetric. For all $\epsilon > 0$, there exists T_0 such that, whenever the time horizon T is longer than $t + T_0$, in order to have $\mathcal{F}(D(1:t)) \neq \emptyset$, the storage size must satisfy:*

$$Q^{\max}_s \geq \frac{\mathrm{Gap}(t)^2}{2}\Big(\frac{1}{R_g - \beta} - \frac{1}{\Delta - \beta}\Big) - \epsilon, \quad (24)$$

where $\mathrm{Gap}(t) = D^{\max}(t) - D^{\min}(t)$. Further, the power limit $\overline{\Phi}_s$ of the storage must satisfy

$$\overline{\Phi}_s \geq \mathrm{Gap}(t)\frac{\Delta - R_g}{\Delta - \beta} - \epsilon. \quad (25)$$

We briefly sketch the idea of the proof. Suppose that the current net-demand is $D(t) = D^{\min}(t)$. We can show that there must exist some $(P_g(t), Q_s(t-1)) \in \mathcal{F}(D(1:t))$ such that $P_g(t) \leq D^{\min}(t)$. Otherwise, we can show that, if $D(t') = D^{\min}(t)$ for all $t' \geq t$, then all future safe-dispatch sets $\mathcal{F}(D(1:t'))$ cannot contain any element with $P_g(t') \leq D(t')$. This contradicts $\mathcal{F}(D(1:t)) \neq \emptyset$ because the storage cannot sustain an infinite period with $P_g(t') > D(t')$. Now, consider the case where the future net-demand keeps increasing at the fastest rate Δ until it reaches the upper bound of net-demand (see Fig. 1c). Since $P_g(t') \leq D^{\min}(t')$, the shaded area then gives a lower bound for $Q_s(t-1) \leq Q^{\max}_s$, which is precisely the right-hand side of (24). Further, the length of the vertical line in Fig. 1c gives a lower bound of (25) for $\overline{\Phi}_s$. Detailed proof is in Appendix A.

B. Sufficient Conditions for $\mathcal{F}(D(1:t)) \neq \emptyset$

Next, we turn to sufficient conditions for $\mathcal{F}(D(1:t)) \neq \emptyset$. Based on the analysis in Section III-A, a natural necessary condition for $\mathcal{F}(D(1:t)) \neq \emptyset$ is that, given $D(t)$, the cropped

leaf-region in Fig. 1b is not empty. In other words, there exists $Q_s(t-1) \in [0, Q_s^{\max}]$ that intersects the cropped leaf-region horizontally, i.e., $h(D(1:t), Q_s(t-1)) \neq \emptyset$, where

$$\begin{aligned} &h(D(1:t), Q_s(t-1)) \\ &= \Big[\max\Big\{ \max_{t_1 \geq t} \xi_{t_1}^{\min}(D(1:t), Q_s(t-1)), \max_{t_1 \geq t} \gamma_{t_1}^{\min}(D(1:t)) \Big\}, \\ &\min\Big\{ \min_{t_2 \geq t} \xi_{t_2}^{\max}(D(1:t), Q_s(t-1)), \min_{t_2 \geq t} \gamma_{t_2}^{\max}(D(1:t)) \Big\} \Big]. \end{aligned} \tag{26}$$

Unfortunately, we can find examples such that this necessary condition is insufficient for reliability. The reason is that the value of $Q_s(t-1)$ is determined by the previous decision $P_g(t-1)$, i.e., $Q_s(t-1) = Q_s(t-2) + P_g(t-1) - D(t-1)$ (cf. (6) and (7)). Thus, even though the "cropped leaf-region" is non-empty, this particular value of $Q_s(t-1)$ may not intersect the cropped leaf-region. As a result, no feasible $P_g(t)$ can ensure future reliability. We note that this situation is in sharp contrast to [10] where similar necessary conditions were shown to be sufficient for the two-generator case. A key difference from [10] is that the safe-dispatch set for the two-generator case in [10] can be taken as 1-dimensional, while ours is 2-dimensional, which thus creates new difficulties. Our key contribution, which is presented below, is to introduce a new flat-top/flat-bottom property of the cropped leaf-region, which is useful for checking reliability. Before we present our sufficient conditions, we introduce the following definitions.

Definition 5 (Flat-top/Flat-bottom)**.** A non-empty "cropped leaf-region" given by conditions (18)-(19) and (22)-(23) is *"flat-top"* if the horizontal line $Q_s(t-1) = Q_s^{\max}$ intersects the "leaf-region", i.e.,(26) holds with $Q_s(t-1) = Q_s^{\max}$. Similarly, it is *"flat-bottom"* if the horizontal line $Q_s(t-1) = 0$ intersects the "leaf-region", i.e.,(26) holds with $Q_s(t-1) = 0$.

Fig. 1b gives an example of "cropped leaf-region" being both "flat-top" and "flat-bottom". Thanks to the convexity of the "leaf-region", a direct benefit of being both "flat-top" and "flat-bottom" is that, for all $Q_s(t-1) \in [0, Q_s^{\max}]$, there always exists a non-empty set of choices for $P_g(t)$. Thus, the difficulty described earlier due to the coupling between $Q_s(t-1)$ and $P_g(t-1)$ is avoided. The following theorem, which is the first main result of our work, then shows that this property is sufficient for reliability.

Theorem 6. *Given $D(1:t)$, if, for all $t' \geq t$ and every $D(t') \in \mathcal{D}_{t'|D(1:t)}$, the "cropped leaf-regions" are both "flat-top" and "flat-bottom", there must exist a causal and robust real-time dispatch algorithm π. Further, the algorithm π may choose any dispatch decision $(P_g(t), Q_s(t))$ from the following set*

$$\begin{aligned} \mathcal{F}' = \{(P_g(t), Q_s(t)) \big| &P_s(t) \in h(D(1:t), Q_s(t-1)), \\ &Q_s(t) = P_g(t) + Q_s(t-1) - D(t)\}. \end{aligned} \tag{27}$$

where $h(D(1:t), Q(t-1))$ is the 1-dimensional interval as described in (26)*.*

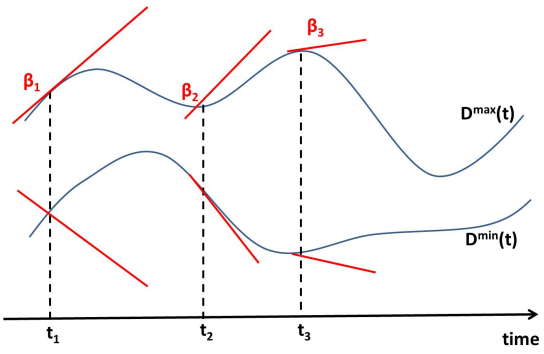

Fig. 2. Using Theorem 7 for general uncertainty sets.

Sketch of Proof. By the flat-top/flat-bottom assumption, the set $h(D(1:t), Q_s(t-1))$, and thus $\mathcal{F}'$s must be non-empty. Suppose that a vector $(P_g(t), Q_s(t))$ is chosen from $\mathcal{F}'$. It follows from the equality $Q_s(t) = P_g(t) + Q_s(t-1) - D(t)$ that such a decision pair $(P_g(t), Q_s(t))$ can balance the net-demand $D(t)$ at time t. We next show the reliability for all future $t' > t$ by constructing a causal real-time dispatch algorithm π that is robust given $D(1:t)$. Algorithm π essentially picks a dispatch level from the interval $h(D(1:t'), Q_s(t'-1))$, while satisfying the generator's ramping constraint from $P_g(t'-1)$. The detailed proof for the sufficiency of the algorithm can be found in Appendix B. □

Remark: We note that Theorem 6 is crucial for the rest of the analysis in this section because it successfully breaks the coupling between time t and $t-1$. Instead, in order to ensure $\mathcal{F}(D(1:t)) \neq \emptyset$, we only need to check the cropped leaf-region at time t, and we do not need to worry about what the previous dispatch decisions were. This decoupling significantly simplifies the analysis. As we will see later, this only incurs a minor loss of optimality because under certain circumstances, the resulting sufficient conditions are tight.

We note that the flat-top/flat-bottom property in Theorem 6 is still tedious to check because we need to check it for every value of $D(t')$. Next, we return to the special case where the upper/lower bounds of net-demand are linear and symmetric (see Lemma 4 and Fig. 1c). Interestingly, here the situation becomes much simpler.

Theorem 7. *Given the uncertainty set $\mathcal{D}$ with symmetric bounds (parameterized by β), the "cropped leaf-region" at time t for every $D(t)$ is "flat-top" and "flat-bottom" if the storage size $Q_s^{\max}$ and power limit $\overline{\Phi}_s$ satisfy the following: $Q_s^{\max} \geq \frac{\mathrm{Gap}(t)^2}{2}\left(\frac{1}{R_g - \beta} - \frac{1}{\Delta - \beta}\right)$ and $\overline{\Phi}_s \geq \mathrm{Gap}(t)\frac{\Delta - R_g}{\Delta - \beta}$.*

The intuition behind Theorem 7 is that in this special setting, the flat-top/flat-bottom property is most difficult to hold when $D(t) = D^{\min}(t)$ (or $D(t) = D^{\max}(t)$). Thus, the requirements in Lemma 4 with $\epsilon = 0$ become sufficient. The detailed proof is non-trivial and is available in Appendix C.

For a general uncertainty set with arbitrary upper and lower bounds, the two extreme cases $D(t) = D^{\min}(t)$ or

$D(t) = D^{\max}(t)$ may no longer give the right requirement on $Q_s^{\max}$ and $\overline{\Phi}_s$. However, we can still leverage Theorem 7 to derive a sufficient condition for the flat-top/flat-bottom property. Specifically, at time t, we find the value of β such that a larger uncertainty set with linear and symmetric bounds can contain all possible future trajectories (see Fig 2). This value of β can be found as follows: consider a time-dependent $\beta(t)$ such that

$$\beta(t) \triangleq \max\{\beta^u(t), \beta^l(t)\}, \tag{28}$$

where

$$\beta^u(t) = \max\big\{\max_{t'>t} \frac{D^{\max}(t') - D^{\max}(t)}{t'-t}, 0\big\},$$
$$-\beta^l(t) = \min\big\{\min_{t'>t} \frac{D^{\min}(t') - D^{\min}(t)}{t'-t}, 0\big\}.$$

Plugging $\beta(t)$ and $\mathrm{Gap}(t)$ into (24) and (25), and taking a maximum over all time t, we then get a sufficient condition for the storage size and power limit for the general case:

$$Q_s^{\max} = \max_t \Big[\frac{\mathrm{Gap}(t)^2}{2}\big(\frac{1}{R_g - \beta(t)} - \frac{1}{\Delta - \beta(t)}\big)\Big], \tag{29}$$

$$\overline{\Phi}_s = \max_t \Big[\mathrm{Gap}(t)\frac{\Delta - R_g}{\Delta - \beta(t)}\Big]. \tag{30}$$

C. Discussion & Comparison with Prior Work

Comparing Theorem 7 with Lemma 4, we can see that our characterization of the safe-dispatch set is quite precise. Indeed, when both $D^{\max}(t)$ and $D^{\min}(t)$ are constant (i.e., $\beta = 0$) and the time horizon approaches infinity, the conditions in Theorem 7 are both sufficient and necessary for $\mathcal{F}(D(1:t)) \neq \emptyset$. To the best of our knowledge, this is the first time in the literature where storage requirement for reliability under multi-stage uncertainty is characterized in such a precise manner. Specifically, note that if there was no storage (i.e., only one generator g), its ramp speed R_g must be at least Δ. Storage allows us to use a generator with $R_g < \Delta$, and the condition in Theorem 7 precisely quantifies the storage needs. In particular, as R_g decreases and Δ increases, the storage capacity $Q_s^{\max}$ also increases. If $\overline{\Phi}_s$ is very large, as Δ approaches infinity, the storage capacity $Q_s^{\max}$ approaches $\frac{\mathrm{Gap}(t)^2}{2}\frac{1}{R_g - \beta}$, which is still a finite value. These results thus provide useful and new insights for storage operations in future power grid with high renewable uncertainty.

A highly desirable feature of the above sufficient conditions is that they do not depend on the time horizon T. In contrast, we have found that, if renewable curtailment is not allowed, using affine policies as in [9] may require storage capacity that grows linearly in T. To see this, suppose that $\mathrm{Gap}(t) = D^{\max}(t) - D^{\min}(t) \geq G$ for all t. The affine policy in [9] sends a fixed fraction η of uncertain demand to the storage. If curtailment is not allowed, the storage size $Q_s^{\max}$ must then be at least $\frac{G}{2}\eta T$, so that it will not over-charge or under-charge under all possible net-demand sequences. If $R_g < \Delta$, the fraction η cannot be too small. The storage capacity must then grow linearly with T. Even if curtailment is allowed, the above analysis suggests that, given $Q_s^{\max}$, the fraction η has to be small when T is large. If $R_g < \Delta$, this small η implies that a considerable fraction of the renewable supply must be curtailed. These observation will be verified by our simulation results in Section V.

In summary, for the scenario of one generator-storage pair, we have provided sufficient conditions for $\mathcal{F}(D(1:t)) \neq \emptyset$, which both answer the RAC problem (by checking $\mathcal{F}(\emptyset) \neq \emptyset$) and the real-time dispatch problem (by dispatching decisions according to Theorem 6). We exploit the complementary characteristics of generator and storage, thus resulting into more effective use of storage units than purely affine policies (as in [9]).

D. Accounting for the Efficiency Loss of Storage Unit

Although throughout the paper we assume no efficiency loss in charging/discharging, we believe that our analysis can also be extended to incorporate efficiency loss. Basically, the quantity $Q_s(t-1) - Q_s(t')$ in (16) needs to be either multiplied or divided by the efficiency ratio. Suppose that the storage unit has efficiency losses in charging and discharging, with efficiency ratio θ_{char} and θ_{disc}, respectively. Then, the conditions (16) and (17) will become

$$\sum_{\tau=t}^{t'} \overline{P}_g^{\mathrm{eff}}(\tau) + \theta_{\mathrm{disc}}(Q_s(t-1) - Q_s(t')) \geq \sum_{\tau=t}^{t'} \max_{D(\tau)\in\mathcal{D}_{\tau|D(1:t)}} \{D(\tau)\}, \tag{31}$$

and

$$\sum_{\tau=t}^{t'} \underline{P}_g^{\mathrm{eff}}(\tau) + \frac{Q_s(t-1) - Q_s(t')}{\theta_{\mathrm{char}}} \leq \sum_{\tau=t}^{t'} \min_{D(\tau)\in\mathcal{D}_{\tau|D(1:t)}} \{D(\tau)\}. \tag{32}$$

It turns out that when $\theta_{\mathrm{char}} < 1$ and/or $\theta_{\mathrm{disc}} < 1$, the above conditions are not necessary any more. However, they can still be used to derive a sufficient condition similar to Theorem 6 and Theorem 7. Specifically, we can still define the leaf-region based on (31) and (32) to obtain

$$Q_s(t-1) \geq \frac{1}{\theta_{\mathrm{disc}}}\Big(-\sum_{\tau=t}^{t'}[P_g(t) + (\tau - t)R_g] + \sum_{\tau=t}^{t'} \max_{D(\tau)\in\mathcal{D}_{\tau|D(1:t)}} \{D(\tau)\}\Big) \tag{33}$$

and

$$Q_s(t-1) \leq \theta_{\mathrm{char}}\Big(-\sum_{\tau=t}^{t'}[P_g(t) - (\tau - t)R_g] + \sum_{\tau=t}^{t'} \min_{D(\tau)\in\mathcal{D}_{\tau|D(1:t)}} \{D(\tau)\}\Big) + Q^{\max}. \tag{34}$$

These inequalities can be used to define the "leaf-region" and "cropped leaf-region" as in Section III-A. Then, we can show a corresponding version of Theorem 6 that, if the "cropped leaf-region" is flat-top and flat-bottom at every time t' given any net-demand $D(t')$, we must then have $\mathcal{F}(D(1:t)) \neq \emptyset$.

Further, we can establish a sufficient condition on the storage size and power limit similar to Theorem 7 that

$$Q_s^{\max} \geq \frac{\mathrm{Gap}(t)^2}{2\theta_{\mathrm{disc}}}\left(\frac{1}{R_g-\beta}-\frac{1}{\Delta-\beta}\right),$$
$$\overline{\Phi}_s \geq \frac{\mathrm{Gap}(t)(\Delta-R_g)}{\theta_{\mathrm{disc}}(\Delta-\beta)}.$$

We note that we only have θ_{disc} in these sufficient conditions because, when there is an balance between $D(t)$ and $P_g(t)$, although $\theta_{\mathrm{disc}} < 1$ *increases* the amount of storage capacity needed for *discharging*, $\theta_{\mathrm{char}} < 1$ actually *decreases* the amount of storage capacity needed for *charging*. Hence, the effect of θ_{disc} dominates. Finally, we expect this result to also be necessary when the upper/lower bounds of net-demand is linear and symmetric. Details will be presented in the journal version of this paper.

IV. The Multi-bus Scenario

In the multi-bus scenario, characterizing the exact safe-dispatch set $\mathcal{F}(D(1:t))$ is intractable due to high dimensionality. Instead, our focus is on obtaining a subset of the exact safe dispatch set for the general case. By verifying that this subset is non-empty, we can then conclude that the true safe dispatch set $\mathcal{F}(D(1:t))$ is non-empty.

Similar to the *demand splitting* idea in [10], we send fractions of the future net-demand uncertainty to the resources according to pre-computed *splitting factors*. However, in contrast to [9] where uncertainty is sent to each generator and storage unit separately, we propose to send uncertainty to a pair of generator and storage. As we argue in Section III, such pairing can better utilize the complementary characteristics of these two types of resources and support a higher level of uncertainty. However, there may be fewer storage units (e.g., pumped hydro) than generators. This fact motivates us to consider the case of storage sharing, where storage units can be split into multiple *virtual storage units* to pair up with generators to form *virtual generator-storage pairs* (VGSPs). After the pairing, the future uncertainty is sent to each VGSP, and its reliability requirement can be checked using our one-generator-storage-pair result in Section III.

1) Creating VGSPs: In [10], we have proposed the conditions for splitting physical generators into virtual generators. Using the same approach, we can split generator g into multiple virtual generators $\hat{g}^v_{g,s}$, one for each storage unit s. Let $P^{\max}_{\hat{g}^v_{g,s}}$, $P^{\min}_{\hat{g}^v_{g,s}}$ and $R_{\hat{g}^v_{g,s}}$ denote the capacity and ramp limit of these virtual generators. Similarly, we split each storage unit s into multiple virtual storage $\hat{s}^v_{g,s}$, one for each generator g. Denote $Q^{\max}_s$ and Q^{init}_s as total storage capacity and initial storage level, respectively, of storage unit s. Define $Q^{\max}_{\hat{s}^v_{g,s}}$, $Q^{\mathrm{init}}_{\hat{s}^v_{g,s}}$ and $\overline{\Phi}_{\hat{s}^v_{g,s}}$ as the storage capacity, initial storage level and power limit for the virtual storage $\hat{s}^v_{g,s}$. Note that the aggregated capabilities (e.g., storage capacity and power limits, generator capacity and ramp limits) of all virtual units from the same physical unit cannot exceed the corresponding physical capability [10]. Specifically, the virtual generators must satisfy

$$\sum_{s\in\mathcal{S}} P^{\max}_{\hat{g}^v_{g,s}} = P^{\max}_g, \sum_{s\in\mathcal{S}} P^{\min}_{\hat{g}^v_{g,s}} = P^{\min}_g \text{ and } \sum_{s\in\mathcal{S}} R_{\hat{g}^v_{g,s}} = R_g. \tag{35}$$

Also, virtual storage units must satisfy, for $\forall s \in \mathcal{S}$

$$\sum_{g\in\mathcal{G}} Q^{\max}_{\hat{s}^v_{g,s}} = Q^{\max}_s, \sum_{g\in\mathcal{G}} Q^{\mathrm{init}}_{\hat{s}^v_{g,s}} = Q^{\mathrm{init}}_s \text{ and } \sum_{g\in\mathcal{G}} \overline{\Phi}_{\hat{s}^v_{g,s}} = \overline{\Phi}_s. \tag{36}$$

Each virtual storage $\hat{s}^v_{g,s}$ is then paired with virtual generator $\hat{g}^v_{g,s}$ to form a VGSP, denoted $\mathrm{VGSP}_{g,s} = (\hat{g}^v_{g,s}, \hat{s}^v_{g,s})$. Thus, there are $g \times s$ number of such pairs in total. Notice that the physical storage unit where $\hat{s}^v_{g,s}$ is associated might be located at a different bus as virtual generator $\hat{g}^v_{g,s}$. This global sharing of storage capacity leads to higher efficiency of our algorithm.

2) Demand Splitting for VGSP: Consider the following affine policy. At each time $t' \geq t$, we separate the net-demand $D_b(t')$ into two parts:

i Main part: $D^{\mathrm{main}}_b(t') = (D^{\max}_b(t') + D^{\min}_b(t'))/2$;
ii Uncertain part: $D^{\mathrm{uncer}}_b(t') = D_b(t') - D^{\mathrm{main}}_b(t')$.

Then, we dispatch the VGSPs to meet the two parts of the net-demand separately. For the main part, denote the part of demand allocated to $\mathrm{VGSP}_{g,s}$ as $P^{\mathrm{main}}_{\mathrm{VGSP}_{g,s}}(t')$. The dispatch policy requires

$$\sum_{b=1}^{N_b} D^{\mathrm{main}}_b(t') = \sum_{s=1}^{N_s}\sum_{g=1}^{N_g} P^{\mathrm{main}}_{\mathrm{VGSP}_{g,s}}(t'). \tag{37}$$

For the uncertain part, we introduce a splitting factor $\{\eta_{b,g,s}\}_{b\in\mathcal{B},g\in\mathcal{G}}$. For each bus b, η_b is a vector where each element is the fraction of uncertain net-demand to be sent to $\mathrm{VGSP}_{g,s}$. The split is valid when η_b satisfies

$$\sum_{s\in\mathcal{S}}\sum_{g\in\mathcal{G}} \eta_{b,g,s} = 1, \forall b \in \mathcal{B}. \tag{38}$$

Therefore, the total amount of net-demand allocated to $\mathrm{VGSP}_{g,s}$ would be

$$D_{\mathrm{VGSP}_{g,s}}(t') = P^{\mathrm{main}}_{\mathrm{VGSP}_{g,s}}(t') + \sum_{b\in\mathcal{B}} \eta_{b,g,s}(D_b(t') - D^{\mathrm{main}}_b(t')). \tag{39}$$

3) Transmission-line Constraints with VGSP: The transmission constraint (8) must hold for all net-demand at all $t' > t$. It turns out that this constraint is convex with respect to the virtualization and splitting decisions, and hence can be converted to a linear form. See Appendix D for details.

4) Safe Dispatch Subset $\mathcal{F}^{\mathcal{VGSP}}(D(1:t))$: We are now ready to define safe dispatch subset $\mathcal{F}^{\mathrm{VGSP}}(D(1:t))$. So far, we have obtained the parameters to characterize all the splitting among VGSPs. Denote $A(t)$ as the set of parameters to identify the VGSPs and their associated splitting, i.e.,

$$\{\eta_{b,g,s}, P^{\max}_{\hat{g}^v_{g,s}}, P^{\min}_{\hat{g}^v_{g,s}}, R_{\hat{g}^v_{g,s}}, Q^{\max}_{\hat{s}^v_{g,s}}, Q^{\mathrm{init}}_{\hat{s}^v_{g,s}}, \overline{\Phi}_{\hat{s}^v_{g,s}}, P^{\mathrm{main}}_{\mathrm{VGSP}_{g,s}}(t')\}.$$

Then, we can use the sufficient conditions (18)-(19), (22)-(23) and (28)-(30) to check whether the safe dispatch set for each

VGSP$_{g,s}$, denoted by $\mathcal{F}_{g,s}^{A(t)}(D(1:t))$, is non-empty. Notice that each of this $\mathcal{F}_{g,s}^{A(t)}(D(1:t))$ is a collection of 2-tuples $(P_{\hat{g}_{g,s}^v}(t), Q_{\hat{s}_{g,s}^v}(t-1))$, where the second entry is the storage level of the virtual storage associated with virtual generator $\hat{g}_{g,s}^v$ at the beginning of time t.

After obtaining a non-empty safe dispatch set for each VGSP, we need to perform an additional step to map the dispatch decisions of all virtual generators and storage units back to the physical units through $\sum_{g\in\mathcal{G}} Q_{\hat{s}_{g,s}^v}(t) = Q_s(t)$ and $\sum_{s\in\mathcal{S}} P_{\hat{g}_{g,s}^v}(t) = P_g(t)$. In this way, the dispatch decision of all physical units $\{P_g(t), Q_s(t) | g \in \mathcal{G}, s \in \mathcal{S}\}$ after mapping will provide the same power output to the grid to balance the demand. Therefore, the safe dispatch subset $\mathcal{F}^{\text{VGSP}}(D(1:t))$ can be defined as follows:

$\mathcal{F}^{\text{VGSP}}(D(1:t)) = \{[\mathbf{P}(t), \mathbf{Q}(t-1)]$ |there exists $A(t)$ satisfying all conditions (37)-(38) and transmission constraints, and there exists $(P_{\hat{g}_{g,s}^v}(t), Q_{\hat{s}_{g,s}^v}(t-1)) \in \mathcal{F}_{g,s}^{A(t)}(D(1:t))$ for all $g \in \mathcal{G}$, satisfying the mapping in previous paragraph$\}$.

We note that most of the constraints in the above definition are convex except two conditions in Theorem 7, for which we develop another convexification method to obtain a sufficient condition for $\mathcal{F}^{VGSP}(D(1:t)) \neq \emptyset$. For details, see Appendix E.

5) RAC and Real-time Dispatch: With the above characterization of the subset $\mathcal{F}^{\text{VGSP}}(D(1:t))$, we can then perform both RAC decision and real-time dispatch as described in Section III-C.

V. Simulation Results

In this section, we conduct MATLAB simulation to evaluate the performance of our proposed algorithm on a standard IEEE 30-bus power system [13]. The system contains 24 fossil-fuel generators, 1 wind farm (at Bus 3), 1 hydroelectric energy storage unit (at Bus 3), 2 loads (at Bus 2 and Bus 3), and 41 transmission lines.

The 24 traditional generators are of 4 different types. The detailed information about the generators is listed in Table I below. We assume that Bus 1, 2, 13, 22, 23 and 27 are generation buses, each of which might have one or multiple generators on it. (See Table II for details.) in Table II.

TABLE I
LISTS OF GENERATORS

Type	Generator Limit	Ramping Rate	Energy Price
A	540-1080MW	4.05MW/15min	48$/MWh
B	378-540MW	0.675MW/15min	40$/MWh
C	342-810MW	4.05MW/15min	48$/MWh
D	0-180MW	13.5MW/15min	60$/MWh

We use the load data and wind data from the grid database of Elia, Belgium's electricity transmission system operator [11]. For the load (around 7200MW), we evenly split the load data into two parts, and then feed into Bus 2 and Bus 3 accordingly (see Fig. 3). For the renewable, we feed Bus 3 with wind data for the same time period. As load data is generally more predictable than wind data in the scale of ISO operation, we assume that the load is perfectly known at the RAC stage, and the uncertainty is entirely from wind availability. The uncertainty set is modeled by (1) and (2), where the uncertainty parameters are derived from Elia's day-ahead prediction data. Specifically, the wind uncertainty bounds are shown in Fig. 4. Our data for transmission line limits are originally from Matpower 5.1 IEEE 30-bus case file [14]. In order to fit in the scale of renewable and load data (i.e., that of an entire ISO), we increase the limit for each transmission line by 50 times.

In the rest of the section, we conduct our numerical study on two scenarios: one with renewable curtailment and the other without. As system safety is our top concern, we compare our

TABLE II
LOCATIONS OF GENERATORS

Generation Bus	Amount and Types of Generators
Bus 1	2 Type-A, 2 Type-D
Bus 2	1 Type-B, 2 Type-D
Bus 13	2 Type-B, 2 Type-C
Bus 22	2 Type-B, 2 Type-C, 2 Type-D
Bus 23	1 Type-C, 2 Type-D
Bus 27	4 Type-D

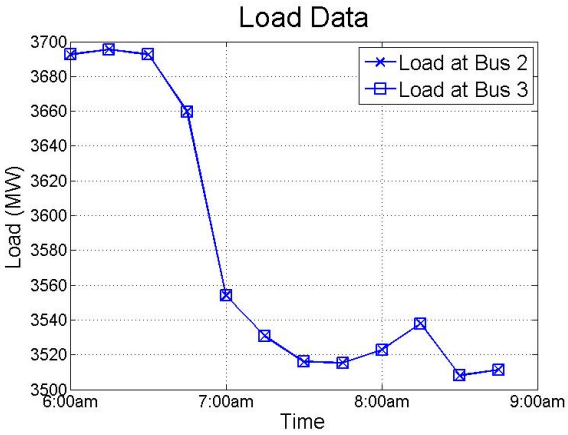

Fig. 3. Load data.

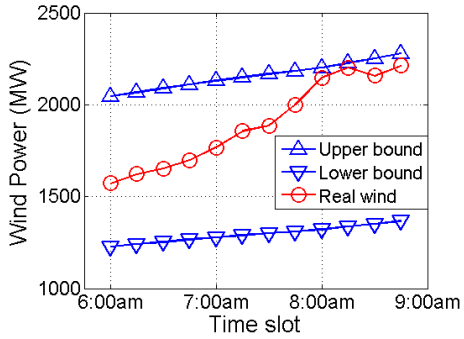

Fig. 4. The uncertainty bounds for wind.

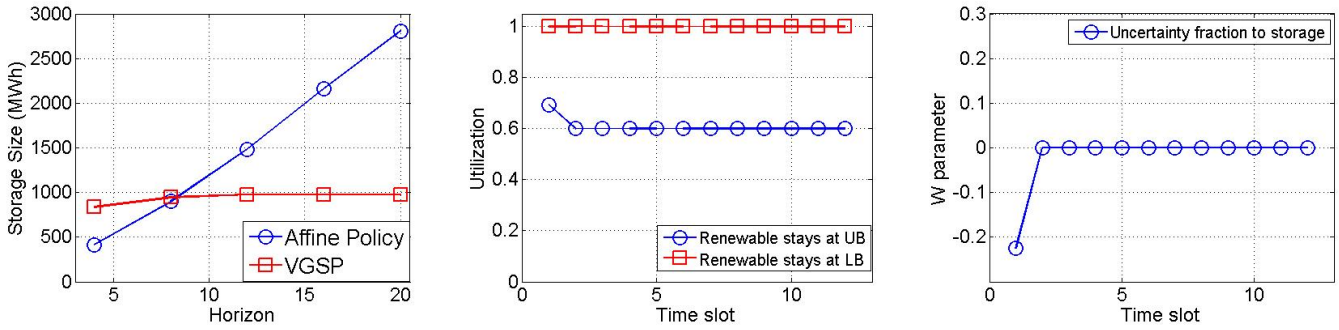

(a) (b) (c)

Fig. 5. (a) The minimum storage size comparison, without renewable curtailment. (b) Renewable utilization levels with curtailment under the affine policy [9]. (c) The fraction of renewable uncertainty sent to storage unit is low under the affine policy [9].

approach with the state-of-art affine policy from [9].

1) When Renewable Curtailment is not Allowed: As mentioned earlier, curtailment of renewable energy wastes natural resources and degrades system economy. Thus, in this section, we assume that renewable curtailment is not allowed. We then use the proposed method to calculate the minimum storage capacity needed so that $\mathcal{F}^{VGSP}(\emptyset) \neq \emptyset$. We also modified the formulation of [9] to disallow renewable curtailment, and find the minimum storage capacity so that there exists an affine policy that satisfies all robust constraints. Fig. 5a compares the minimum storage size needed to ensure reliable grid operations with varying time horizons. For the affine policy [9], we clearly see a drastic increase in storage size as the operation horizon increases. While the storage size needed for VGSP algorithm is rather stable. This result is consistent with our previous discussion (see Section III-C) that storage is better utilized when paired with generators.

2) When Renewable Curtailment is Allowed: When renewable curtailment is allowed, the storage need of the affine policy in [9] will decrease. However, this reduction is usually at the cost of significant renewable curtailment. To illustrate this, we set the storage capacity on Bus 3 to be 1250MWh, which is sufficient for reliable grid operations under our proposed VGSP algorithm. We then simulate the affine policy of [9] with renewable curtailment.

TABLE III
TOTAL DISPATCH FUEL COST VS RENEWABLE SCALE

Renewable Scale	0.5	0.8	1
Affine($)	853,304	798,373	760,119
VGSP($)	827,494	762,156	723,128
Savings	3.02%	4.54%	4.86%

Fig. 5b shows the renewable utilization level for each time slots under two possible trajectories of renewable realization: one where renewable stays at the upper bound and the other where renewable stays at the lower bound. We can clearly see that, if renewable realization is at its upper bound, the renewable utilization is about 60% most of the time, while all renewable can be utilized if the renewable realization is at the lower bound. This observation suggests that the affine policy in [9] essentially reduces the renewable uncertainty by curtailing renewable when the supply is high. While this curtailment enhances grid reliability, it reduces the utilization level of renewable. As we explained in Section III, this problem will likely be more severe when the time-horizon is long. This observation is further confirmed in Fig. 5c, where we show the fraction of the uncertain part of renewable output that is sent to storage according to the affine policy in [9]. This fraction is close to zero for most time-slots, indicating that the storage is not utilized effectively to overcome renewable uncertainty. In contrast, at the same storage level, our proposed approach can ensure grid reliability with no curtailment.Finally, Table III show that, even with a simple economy dispatch algorithm, our proposed VGSP algorithm leads to lower fuel costs. The economy dispatch algorithm picks a operation point $(\mathbf{P}(t), \mathbf{Q}(t))$ that minimizes the fuel-cost in current operating interval (no look-ahead window is implemented) while satisfying all the robust constraints specified by our proposed VGSP algorithm (see Section IV-5) or the affine policy in [9]. For the affine policy in [9], day-ahead policy parameters $(\mathbf{w}, \mathbf{W})$ are computed based on renewable uncertainty in Fig. 4. In real-time dispatch, the affine policy is guided by the day-ahead computed parameters.

VI. CONCLUSION

We study robust online multi-stage strategies under high renewable uncertainty for power systems with both generators and storage units. For a single-bus system with one generator-storage pair, we characterize necessary conditions and sufficient conditions of "safe dispatch set," which are tight under certain circumstances. For the more general multi-bus scenario, we develop a computationally-efficient approach to obtain a proper subset of the exact safe dispatch set using the idea of VGSP pairing and demand splitting. Our numerical study shows that the proposed VGSP algorithm outperforms the state-of-the-art affine policy in [9]. For future work, we will extend the approach to more general system settings, e.g., with time-varying ramping limits. Further, we will study how

to directly account for economy in the online decisions for both unit-commitment and economic dispatch.

REFERENCES

[1] T. Mai, D. Sandor, R. Wiser, and T. Schneider, "Renewable Electricity Futures Study: Executive Summary," National Renewable Energy Laboratory, Golden, CO, Tech. Rep., 2012.

[2] J. Eyer, G. Corey, and S. N. Laboratories, *Energy Storage for the Electricity Grid: Benefits and Market Potential Assessment Guide*, ser. SAND (Series). Sandia National Laboratories, 2010.

[3] "Order No. 888," FERC, Tech. Rep., 1996.

[4] MISO Energy. [Online]. Available: https://www.misoenergy.org

[5] ISO-NE. [Online]. Available: https://www.iso-ne.org

[6] D. Bertsimas, E. Litvinov, X. A. Sun, J. Zhao, and T. Zheng, "Adaptive robust optimization for the security constrained unit commitment problem," *IEEE Trans. on Power Systems*, vol. 28, no. 1, February 2013.

[7] R. Jiang, J. Wang, and Y. Guan, "Robust unit commitment with wind power and pumped storage hydro," *IEEE Transactions on Power Systems*, vol. 27, no. 2, pp. 800–810, 5 2012.

[8] A. Lorca, X. A. Sun, E. Litvinov, and T. Zheng, "Multistage adaptive robust optimization for the unit commitment problem," *Operations Research*, vol. 64, no. 1, pp. 32–51, 2016.

[9] A. Lorca and X. A. Sun, "Multistage robust unit commitment with dynamic uncertainty sets and energy storage," *arXiv preprint arXiv:1604.04890*, 2016.

[10] S. Zhao, X. Lin, D. Aliprantis, H. Villegas, and M. Chen, "Online Multi-stage Decisions for Robust Power-Grid Operations under High Renewable Uncertainty," in *IEEE INFOCOM*, San Francisco, 2016.

[11] Elia. Grid data. [Online]. Available: http://www.elia.be/en/grid-data

[12] A. Wood, B. Wollenberg, and G. Sheble, *Power Generation, Operation, and Control*. Wiley, 2013.

[13] "Power systems test case archive," available at http://www2.ee.washington.edu/research/pstca/.

[14] MATPOWER. [Online]. Available: http://www.pserc.cornell.edu/matpower/

APPENDIX A
PROOF OF LEMMA 4

We first prove (24), and (25) can be shown similarly. We can prove the lemma by contradiction. Let $\epsilon > 0$. We will show that there exists T_0 such that when $T > t + T_0$, the system cannot be safe. Towards this end, suppose that the storage size is strictly less than RHS of (24), i.e.,

$$\hat{Q}_s^{\max} < \frac{\mathrm{Gap}(t)^2}{2}\Big(\frac{1}{R_g-\beta} - \frac{1}{\Delta-\beta}\Big) - \epsilon. \qquad (40)$$

Let the current net-demand be $D(t) = D^{\min}(t)$. Let us consider a possible net-demand sequence that increases from $D^{\min}(t)$ to meet the net-demand upper bound at the fastest rate Δ. As shown in Fig. 1c, it takes $T_{\text{top}} = \frac{\mathrm{Gap}(t)}{R_g-\beta}$ for the generator to ramp from $D^{\min}(t)$ up to the demand upper bound. Notice that the term $Q^* = \frac{\mathrm{Gap}(t)^2}{2}\big(\frac{1}{R_g-\beta} - \frac{1}{\Delta-\beta}\big)$ is the storage size needed if the generator operates at $D^{\min}(t)$. Now, for the storage size specified in (40), there exists δ_ϵ such that $\delta_\epsilon \frac{2\mathrm{Gap}(t)-\delta_\epsilon}{2(R_g-\beta)} = \epsilon$. Then, the generator g has to operate at $P_g(t) \geq D^{\min}(t) + \delta_\epsilon$ so that the area enclosed by the line with slope Δ and the line with slope R_g in Fig. 1c is no greater than the RHS of (40). Now, denote the shortest time for the generator to ramp up from $P_g(t) = D^{\min}(t) + \delta_\epsilon$ to net-demand upper bound as $\hat{T}_{\text{top}}$. Then, we have $\hat{T}_{\text{top}} = \frac{\mathrm{Gap}(t)-\delta_\epsilon}{R_g-\beta}$. Note that, under linear and symmetric net-demand bounds, $D^{\max}(t') \geq D^{\max}(t)$ and $\mathrm{Gap}(t') \geq \mathrm{Gap}(t), \forall t' > t$. Thus, as long as $T > t' + \hat{T}_{\text{top}}$, we must also have

$$P_g(t') \geq D^{\min}(t) + \delta_\epsilon, t' > t.$$

On the other hand, $D(t') = D^{\min}(t), t' > t$ is also a possible future demand sequence. As the generator must operate at $P_g(t') \geq D^{\min}(t)+\delta_\epsilon$, the storage status will always be charging if $D(t') = D^{\min}(t)$ for all $t' > t$. Thus, the storage size in (40) can at most operate for a period of length

$$T_c = \frac{\hat{Q}_s^{\max}}{\delta_\epsilon} < \frac{\mathrm{Gap}(t)^3}{2\epsilon(R_g-\beta)}\big(\frac{1}{R_g-\beta} - \frac{1}{\Delta-\beta}\big).$$

As a result, for $T_0 > T_c + T_{\text{top}}$, the system will be unsafe, which contradicts with our hypothesis. Thus, we have proved (24), i.e., the first part of lemma. As shown in Fig. 1c, (25) follows from (24).

APPENDIX B
PROOF OF THEOREM 6

By the flat-top/flat-bottom assumption, the set $h(D(1:t), Q_s(t-1))$, and thus $\mathcal{F}'$ must be non-empty. Suppose that a vector $(P_g(t), Q_s(t))$ is chosen from $\mathcal{F}'$. It follows from the equality $Q(t) = P(t)+Q(t-1)-D(t)$ that any decision pair $(P_g(t), Q_s(t))$ can balance the net-demand $D(t)$ at time t. We next show the reliability for all future $t' > t$ by constructing a causal real-time dispatch algorithm π that is robust given $D(1:t)$. Consider the algorithm π as follows.

Algorithm π: At any time $t' > t$, first pick any dispatch level for the generator inside the set $P(t') \in h(D(1:t'), Q(t'-1)) \bigcap C(P(t'-1))$, and then determine the storage dispatch decision according to $Q(t') = P(t')+Q(t'-1)-D(t')$. Here, the set $h(D(1:t'), Q(t'-1))$ is defined in the same way as in (26), and $C(P(t'-1))$ is the possible range of the dispatch level that can be reached by the generator given the dispatch level in the previous time slot, i.e.

$$C(P(t'-1)) = \Big[P(t'-1) - R_g, P(t'-1) + R_g\Big]. \qquad (41)$$

In other words, Algorithm π cannot just pick any $P(t') \in h(D(1:t'), Q(t'-1))$, but $P(t')$ must also be reachable from the previous level $P(t'-1)$. According to the definition of Algorithm π, as long as we can show that $h(D(1:t'), Q(t'-1)) \bigcap C(P(t'-1))$ is always non-empty for $\forall t' > t$, and the storage charing/discharging power $\Phi(t') = Q(t') - Q(t'-1)$ is always in the range of $[-\overline{\Phi}_s, \overline{\Phi}_s]$, Algorithm π will balance the demand $D(t')$ for all $t' > t$, and thus guarantee the safety of the system. Hence, we prove the above algorithm is robust given $D(1:t)$ and $\mathbf{P}(t)$ based on the following claims:

C1. $h(D(1:t'), Q(t'-1)) \neq \emptyset, \forall t' \geq t$;
C2. $-\overline{\Phi}_s \leq Q(t') - Q(t'-1) \leq \overline{\Phi}_s$, and $Q(t') \in [0, Q^{\max}]$;
C3. $h(D(1:t'), Q(t'-1)) \bigcap C(P(t'-1)) \neq \emptyset, \forall t' > t$.

To see why C1-C3 is sufficient , note that C1 and C2 guarantee the supply-demand balance constraint (7), while C3 ensures that the generator ramping constraints (4) are obeyed.

A. Proof of Claim C1

Based on (26), we can check the non-emptiness of $h(\cdot,\cdot)$ by comparing the interval boundaries. Thus, it is sufficient to show that the following inequalities hold:

i) $\xi^{\min}_{t_1}(D(1:t'),Q(t'-1)) \le \xi^{\max}_{t_2}(D(1:t'),Q(t'-1))$, for $\forall t_1,t_2 \ge t'$
ii) $\xi^{\min}_{t_1}(D(1:t'),Q(t'-1)) \le \gamma^{\max}_{t_2}(D(1:t')), \forall t_1 \ge t'$;
iii) $\xi^{\max}_{t_2}(D(1:t'),Q(t'-1)) \ge \gamma^{\min}_{t_1}(D(1:t')), \forall t_2 \ge t'$.

1) Proof of i): Recall that $\max_{t_1}\gamma^{\min}_{t_1}(D(1:t'),Q(t'-1))$ and $\min_{t_2}\gamma^{\max}_{t_2}(D(1:t'),Q(t'-1))$ are the left and right boundaries, respectively, of the "leaf-region" when $Q=Q(t'-1)$. Thus, (i) follows if we can find P such that $(P,Q(t'-1))$ belongs to the "leaf-region". This existence follows from the flat-top/flat-bottom conditions, i.e., (26) holds for $Q_s(t-1)=Q^{\max}_s$ and $Q_s(t-1)=0$, and the fact that the leaf-region is a convex set. Specifically, by the flat-top condition, there exists P_{full} such that

$$\max_{t_1}\xi^{\min}_{t_1}(D(1:t'),Q^{\max}) \le P_{\text{full}} \le \min_{t_2}\xi^{\max}_{t_2}(D(1:t'),Q^{\max}).$$

Similarly, from the flat-bottom condition, there exist P_{empty} such that

$$\max_{t_1}\xi^{\min}_{t_1}(D(1:t'),0) \le P_{\text{empty}} \le \min_{t_2}\xi^{\max}_{t_2}(D(1:t'),0).$$

Let $\alpha=\frac{Q(t'-1)}{Q^{\max}}$. Note that $0\le\alpha\le 1$. Let $P=\alpha P_{\text{full}}+(1-\alpha)P_{\text{empty}})$. Then $(P,Q(t'-1))$ must also belong to the convex leaf-region. Property (i) then follows.

2) Proof of ii) and iii): As the "cropped leaf-region" is flat-top and flat-bottom, the following inequalities will hold:

$$\max_{t_1}\xi^{\min}_{t_1}(D(1:t'),0) \le \min_{t_2}\gamma^{\max}_{t_2}(D(1:t')),$$
$$\min_{t_2}\xi^{\max}_{t_2}(D(1:t'),Q^{\max}) \ge \max_{t_1}\gamma^{\min}_{t_1}(D(1:t')).$$

From (20), it implies that, for $\forall Q(t'-1)\in[0,Q^{\max}]$,

$$\begin{aligned}\max_{t_1}\xi^{\min}_{t_1}(D(1:t'),Q(t'-1)) &\le \max_{t_1}\xi^{\min}_{t_1}(D(1:t'),0)\\ &\le \min_{t_2}\gamma^{\max}_{t_2}(D(1:t')),\end{aligned}$$

which is precisely ii).

Similarly, iii) can be shown by

$$\begin{aligned}\min_{t_2}\xi^{\max}_{t_2}(D(1:t'),Q(t'-1)) &\ge \min_{t_2}\xi^{\max}_{t_2}(D(1:t'),Q^{\max})\\ &\ge \max_{t_1}\gamma^{\min}_{t_1}(D(1:t')).\end{aligned}$$

B. Proof of Claim C2

As mentioned above, under storage power limit $\overline{\Phi}_s$, the generator dispatch level at t' has to satisfy

$$\max_{t_1}\gamma^{\min}_{t_1}(D(1:t')) \le P(t') \le \min_{t_s}\gamma^{\max}_{t_2}(D(1:t')).$$

From the expression of $\gamma^{\min}_{t_1}(\cdot)$ and $\gamma^{\max}_{t_2}(\cdot)$, when $t_1=t_2=t'$, the above inequality implies that,

$$D(t')-\overline{\Phi}_s \le P(t') \le D(t')+\overline{\Phi}_s,$$

For time t', supply-demand has to be balanced by

$$P(t')+Q(t'-1)-Q(t')=D(t').$$

Thus, the inequalities follows

$$-\overline{\Phi}_s \le Q(t'-1)-Q(t') \le \overline{\Phi}_s, \forall t' \ge t.$$

To see $Q(t')\le Q^{\max}$, notice that by $P_g(t')\in h(D(1:t),Q_s(t-1))$, (15) must hold. Thus, the following is true at time t',

$$P(t') \le -Q(t'-1)+Q^{\max}+D(t')$$

We then have

$$\begin{aligned}Q(t') &= P(t')+Q(t'-1)-D(t')\\ &\le Q^{\max}.\end{aligned}$$

Similarly, (20) implies that $Q(t')\ge 0$, and Claim C2 follows.

C. Proof of Claim C3

In order to show that

$$h(D(1:t'),Q(t'-1))\bigcap C(P(t'-1)) \ne \emptyset, \forall t' > t, \quad (42)$$

we use mathematical induction. Define $C(P(t-1)) = [P^{\min}_g, P^{\max}_g]$ to be entire power range of the generator. Then, the induction is described as follows.

- Initial Step: when $t'=t$, the intersection is just $h(D(1:t),Q(t-1))$, which is non-empty as shown in Claim C1. Hence, the statement (42) holds trivially;
- Induction Step: suppose that at time $t'-1\ge t$, $h(D(1:t'-1),Q(t'-2))\bigcap C(P(t'-2))\ne\emptyset$. We next show that the statement (42) is also true for time t', i.e., at time t', we need to show that

$$h(D(1:t'),Q(t'-1))\bigcap C(P(t'-1))\ne\emptyset.$$

To show the induction step, we can equivalently prove that

$$\begin{aligned}P(t'-1)+R_g \ge \max\Big\{ &\max_{t_1}\big\{\xi^{\min}_{t_1}(D(1:t'),Q(t'-1))\big\},\\ &\gamma^{\min}_{t_1}(D(1:t'-1))\Big\}, \quad (43)\end{aligned}$$

and

$$\begin{aligned}P(t'-1)-R_g \le \min\Big\{ &\min_{t_2}\big\{\xi^{\max}_{t_2}(D(1:t'),Q(t'-1))\big\},\\ &\gamma^{\max}_{t_2}(D(1:t'-1))\Big\}. \quad (44)\end{aligned}$$

Once we show that the above two inequalities hold for any $P(t'-1)\in h(D(1:t'-1),Q(t'-2))$, we can guarantee that, given decision $P(t'-1)$, the generator is able to ramp to some $P(t')\in h(D(1:t'),Q(t'-1))$. Here, we only focus on proving (43). Inequality (44) can be proved in similar way. Hence, it is sufficient to show that

$$\begin{aligned}&\max\Big\{\max_{t_1\ge t'-1}\big\{\xi^{\min}_{t_1}(D(1:t'-1),Q(t'-2))\big\},\gamma^{\min}_{t_1}(D(t'-1))\Big\}\\ &+R_g \ge \max\Big\{\max_{t_1\ge t'}\big\{\xi^{\min}_{t_1}(D(1:t'),Q(t'-1))\big\},\gamma^{\min}_{t_1}(D(1:t'))\Big\}.\end{aligned} \quad (45)$$

To prove (45), notice that we can compare $\xi_{t_1}^{\min}(\cdot)$ term and $\gamma_{t_1}^{\min}(\cdot)$ term separately. Hence, it is sufficient to show that

$$\max_{t_1\geq t'}\left\{\xi_{t_1}^{\min}(D(1:t'-1),Q(t'-2))\right\}+R_g \geq \max_{t_1\geq t'}\left\{\xi_{t_1}^{\min}(D(1:t'),Q(t'-1))\right\}, \quad (46)$$

and

$$\max_{t_1\geq t'}\left\{\gamma_{t_1}^{\min}(D(1:t'-1)\right\}+R_g \geq \max_{t_1\geq t'}\gamma_{t_1}^{\min}(D(1:t')). \quad (47)$$

We first prove (46). For $\forall t_1 \leq t'$, it suffices to prove

$$P(t'-1)+R_g \geq \xi_{t_1}^{\min}(D(1:t'),Q(t'-1)), \quad (48)$$

where

$$P(t'-1) \geq \xi_{t_1}^{\min}(D(1:t'-1),Q(t'-2)). \quad (49)$$

Multiplying both sides by $(t_1-t'+1)$, (48) is equivalent to

$$\begin{aligned}&\sum_{\tau=t'}^{t_1}(P(t'-1)+R_g)\\ &\geq -\sum_{\tau=t'}^{t_1}(\tau-t')R_g - Q(t'-1)+\sum_{\tau=t'}^{t_1}\max_{D(\tau)\in\mathcal{D}_{\tau|D(1:t')}}D(\tau),\end{aligned}$$

which is in turn equivalent to

$$\begin{aligned}&\sum_{\tau=t'}^{t_1}\left[(P(t'-1)+R)+(\tau-t')R\right]+Q(t'-1)\\ &=\sum_{\tau=t'}^{t_1}\left[P(t'-1)+(\tau-t')R\right]+Q(t'-1) \quad (50)\\ &\geq \sum_{\tau=t'}^{t_1}\max_{D(\tau)\in\mathcal{D}_{\tau|D(1:t')}}D(\tau).\end{aligned}$$

Similarly, (49) is equivalent as

$$\sum_{\tau=t'-1}^{t_1}\left[P(t'-1)+(\tau-t'+1)R\right]+Q(t'-2)-D(t'-1) \geq \sum_{\tau=t'-1}^{t_1}\max_{D(\tau)\in\mathcal{D}_{\tau|D(1:t'-1)}}D(\tau). \quad (51)$$

As $Q(t'-1)=P(t'-1)+Q(t'-2)-D(t'-1)$, we have

$$\begin{aligned}\text{LHS of (50)} &= \sum_{\tau=t'}^{t_1}\left[P(t'-1)+(\tau-t'+1)R\right]\\ &\quad +P(t'-1)+Q(t'-2)-D(t'-1)\\ &=\sum_{\tau=t'-1}^{t_1}\left[P(t'-1)+(\tau-t'+1)R\right]\\ &\quad +Q(t'-2)-D(t'-1)\\ &\geq \sum_{\tau=t'-1}^{t_1}\max_{D(\tau)\in\mathcal{D}_{\tau|D(1:t'-1)}}D(\tau)-D(t'-1)\\ &\qquad\qquad\text{(Using (51))}\\ &\geq \sum_{\tau=t'-1}^{t_1}\max_{D(\tau)\in\mathcal{D}_{\tau|D(1:t')}}D(\tau)-D(t'-1)\\ &\geq \sum_{\tau=t'}^{t_1}\max_{D(\tau)\in\mathcal{D}_{\tau|D(1:t')}}D(\tau),\end{aligned}$$

where the second-to-last inequality holds because the uncertainty of $D(\tau)$ reduces as time evolves from $t'-1$ to t', i.e., $\mathcal{D}_{\tau|D(1:t')}\subset\mathcal{D}_{\tau|D(1:t'-1)}$. Thus we have proved (50), which implies (46).

The remaining inequality (47) can be shown as follows, for $\forall t_1\geq t'$,

$$\begin{aligned}&\gamma_{t_1}^{\min}(D(1:t'))\\ &=\max_{D(t')\in\mathcal{D}_{t'|D(1:t)}}\{D(t')\}-(t_1-t')R_g-\overline{\Phi}_s\\ &\leq \max_{D(t_1)\in\mathcal{D}_{t_1|D(1:t'-1)}}\{D(t')\}-(t_1-(t'-1))R_g-\overline{\Phi}_s+R_g\\ &=\gamma_{t_1}^{\min}(D(1:t'-1))+R_g.\end{aligned}$$

Thus, we have proved (43), and (44) can be shown in similar way. By induction, we have proved Claim C3, which completes the entire proof.

Appendix C
Proof of Theorem 7

We can prove the theorem in the following two steps:

i) the original uncropped "leaf-regions" given by (20) and (21) for every $D(t)$ is both flat-top and flat-bottom;
ii) the "cropped leaf-region" cut by (22) and (23) will retain the flat-top/flat-bottom property.

The results of Lemma 8 and Lemma 9 precisely show these two steps. Once we prove the lemmas, the correctness of the theorem follows. Next, we proceed to prove the lemmas.

Lemma 8. *Given the uncertainty set $\mathcal{D}$ with symmetric bounds (parameterized by β), the uncropped "leaf-region" for every $D(t)$ is "flat-top" and "flat-bottom" if the storage size satisfies the minimum requirement*

$$Q_s^{\max}\geq\frac{\mathrm{Gap}(t)^2}{2}\left(\frac{1}{R_g-\beta}-\frac{1}{\Delta-\beta}\right). \quad (52)$$

.

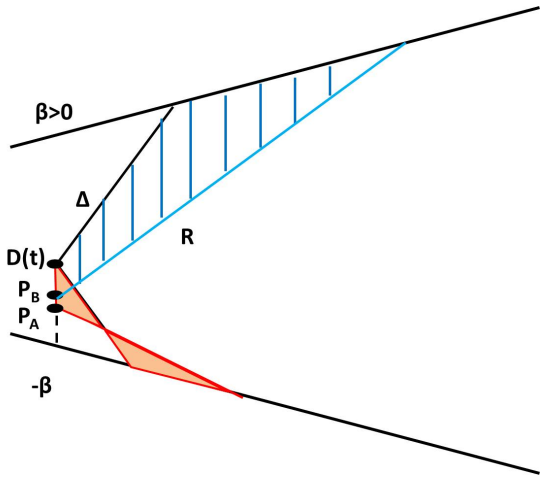

Fig. 6. An illustration of the movement of A and B according to net-demand increase δ.

Proof. Suppose the bounds of net-demand $D^{\max}(\cdot)$ and $D^{\min}(\cdot)$ are changing at rate β and $-\beta$, respectively. We first prove "flat-top", and the "flat-bottom" part can be shown easily by symmetric argument.

Flat-top proof: Given the uncertainty set $\mathcal{D}$ and generator ramping speed R_g, the "leaf-region" at time t' is determined by $D(t') \in \mathcal{D}_{t'|D(1:t)}$ through constraints (18) and (19). Thus the "flat-top" statement can be proved by showing the following:

i) The "leaf-region" for $D(t') = \min\{\mathcal{D}_{t'|D(1:t)}\}$ is "flat-top";

ii) If the "leaf-region" regarding any $D(t') \in \mathcal{D}_{t'|D(1:t)}$ is "flat-top", then with arbitrarily small increase δ in net-demand, the "leaf-region" for $(D(t') + \delta)$ is "flat-top".

One can easily see that i) is true using the interpretation of curves from condition (18) and (19) when the minimum storage requirement in (52) is met. As mentioned before, every point on red concave curve represents an operation point where the storage has just enough space to accommodate decreasing net-demand. Thus, $(D^{\min}(t'),Q_s^{\max})$ will belong to red concave curve because the future decreasing net-demand can be met by just ramping down the generator. Also, point $(D^{\min}(t'),Q_s^{\max})$ will be on or above blue convex curve. Note that if (52) is met with an equal sign, we get a barely "flat-top" case where $Q(t-1) = Q_s^{\max}$ line only intersects "leaf-region" at one point $(D^{\min}(t'),Q_s^{\max})$.

The next proof of ii) is the key component of the theorem. Suppose that the uncertainty bounds is increasing, i.e. $\beta > 0$. The decreasing-bound case is a symmetric scenario and can be proved using same approach. As shown in Fig. 1b, let A and B denote the points where $Q(t'-1) = Q_s^{\max}$ line intersects the red concave curve and blue convex curve, respectively. Since the "leaf-region" corresponding to $D(t')$ is flat-top, point A is to the right of point B. If net-demand increases, both points A and B will move along the $Q(t-1) = Q_s^{\max}$ line to the right. In order to establish property ii), it suffices to show that, with tiny increase δ in net-demand, the speed that A moves to the right is quicker than the speed of B.

The interpretation of point A is the operation point that the storage does not require any charge-in space for the future decreasing demand. As shown in Fig. 6, the point A refers to an operation point such that the two red triangles have the same area. Thus the generator power level P_A at point A will satisfy

$$\frac{1}{2}\frac{(D - D^{\min})^2}{\Delta - \beta} = \frac{1}{2}\frac{(P_A - D^{\min})^2}{R_g - \beta}. \tag{53}$$

To get the rate of change on P_A with respect to D, we can differentiate on both sides and get

$$\begin{aligned}\frac{dP_A}{dD} &= \frac{D - D^{\min}}{P_A - D^{\min}}\frac{R_g - \beta}{\Delta - \beta} \\ &\overset{\text{eqn (53)}}{=} \sqrt{\frac{\Delta - \beta}{R_g - \beta}\frac{R_g - \beta}{\Delta - \beta}} \\ &= \sqrt{\frac{R_g - \beta}{\Delta - \beta}}.\end{aligned} \tag{54}$$

Now we look at the rate of change of point B. The interpretation of point B is the operation point that the storage has just enough energy to support increasing net-demand. In Fig. 6, it is represented as the area of blue shaded region being equal to $Q^{\max}$, i.e.

$$\frac{1}{2}\frac{(D^{\max} - P_B)^2}{R_g - \beta} = \frac{1}{2}\frac{(D^{\max} - D)^2}{\Delta - \beta} + Q^{\max}. \tag{55}$$

Similar to (54), we can differentiate on both sides of (55) and get

$$\begin{aligned}\frac{dP_B}{dD} &= \frac{D^{\max} - D}{D^{\max} - P_B}\frac{R_g - \beta}{\Delta - \beta} \\ &\le \frac{R_g - \beta}{\Delta - \beta},\end{aligned} \tag{56}$$

where the last inequality comes from the fact that $P_B \le D$, and thus $\frac{D^{\max} - D}{D^{\max} - P_B} \le 1$. As $0 \le \beta \le R \le \Delta$, we have the following chain of inequalities:

$$\frac{dP_B}{dD} \le \frac{R_g - \beta}{\Delta - \beta} \le \sqrt{\frac{R_g - \beta}{\Delta - \beta}} = \frac{dP_A}{dD},$$

and the statement ii) is true. The result of the theorem then follows. □

With power limit of the storage, the feasible range within the "leaf-region" will be cropped to contain only those operation points with $P_g(t) \in [\max_{t_1} \gamma_{t_1}^{\min}(D(1:t)), \min_{t_2} \gamma_{t_2}^{\max}(D(1:t))]$. However, such cutting still retains the "top&bottom-flatness" of the "leaf-region", as we will prove in the following lemma.

Lemma 9 (Top&bottom Flatness with Storage Power Limit)**.** *Given the uncertainty set $\mathcal{D}$ with symmetric bounds (parameterized by β), if the uncropped "leaf-region" is always flat-top/flat-bottom, $Q_s^{\max}$ satisfies* (52) *and $\overline{\Phi}_s$ satisfies*

$$\overline{\Phi}_s \ge \text{Gap}(t)\frac{\Delta - R_g}{\Delta - \beta}, \tag{57}$$

the "cropped leaf-region" due to storage power limit $\overline{\Phi}_s$ is still flat-top and flat-bottom.

Proof. We first prove the "flat-top" part, and the "flat-bottom" statement can be proved in a similar way. Similar to the proof of Lemma 8, we define point C as $(P_c, Q_s^{\max})$, where $P_C = \max_{t_1} \gamma_{t_1}^{\min}(D(1:t))$. We can then show the lemma by comparing the rate of change of point A (defined in the proof of Lemma 8) and that of point C, as the current net-demand $D(t) = D$ increases. Specifically, to show that the uncropped "leaf-region" is flat-top, it is sufficient to show that

$$\frac{dP_C}{dD} \leq \frac{dP_A}{dD}. \tag{58}$$

As shown in Fig. 6, it takes t_C time for demand to increase from $D(t) = D$ to meet its upper bound, where

$$t_C = \frac{D^{\max} - D}{\Delta - \beta}.$$

By the definition of P_C, at time $t + t_C$, the power limit $\overline{\Phi}_s$ of the storage must satisfy

$$\begin{aligned}\overline{\Phi}_s &= D - P_C + (\Delta - R_g)t_C \\ &= D - P_C + \frac{\Delta - R_g}{\Delta - \beta}(D^{\max} - D).\end{aligned}$$

To get the rate of change of P_C with respect to D, we can differentiate on both sides and get

$$\begin{aligned}\frac{dP_C}{dD} &= 1 - \frac{\Delta - R_g}{\Delta - \beta} \\ &= \frac{R_g - \beta}{\Delta - \beta} \\ &\leq \sqrt{\frac{R_g - \beta}{\Delta - \beta}} \qquad \text{(since } R_g \leq \Delta\text{, hence } \tfrac{R_g - \beta}{\Delta - \beta} \leq 1\text{)} \\ &= \frac{dP_A}{dD}. \qquad \text{(using (54))}\end{aligned}$$

□

APPENDIX D
TRANSMISSION CONSTRAINTS FOR MULTI-BUS SCENARIO

In the DC power model, the power flow on transmission line l is a linear combination of the net bus injection on each bus, i.e.

$$|f_l(t')| = \left| \sum_{b=1}^{N_b} S_{l,b}\Big(D_b(t') - \sum_{g\in\mathcal{G}_b} P_g(t') - \sum_{s\in\mathcal{S}_b} \Phi_s(t')\Big)\right| \leq TL_l.$$

Note that we need to ensure that the above inequality holds for any splitting of demand to the virtual generator-storage pair. There are in fact two levels of splitting. To see this, consider the bus injection on bus b at t',

$$\begin{aligned}J_b(t') &= D_b(t') - \sum_{g\in\mathcal{G}_b} P_g(t') - \sum_{s\in\mathcal{S}_b} \Phi_s(t') \\ &= D_b(t') - \sum_{(g,s):g\in\mathcal{G}_b} P_{\hat{g}^v_{g,s}}(t') - \sum_{(g,s):s\in\mathcal{S}_b} \Phi_{\hat{s}^v_{g,s}}(t').\end{aligned} \tag{59}$$

For each $VGSP_{g,s}$, the following must hold

$$D_{VGSP_{g,s}}(t') = P_{\hat{g}^v_{g,s}}(t') + \Phi_{\hat{s}^v_{g,s}}(t'). \tag{60}$$

From (59) and (60), we can see that there are two layers of splitting happening in the system: 1) the first layer splits net-demand onto VGSPs, i.e., $D_{VGSP_{g,s}}$; and 2) the second layer splits each VGSP demand onto the virtual generator and the virtual storage unit, i.e., between $P_{\hat{g}^v_{g,s}}(t')$ and $\Phi_{\hat{s}^v_{g,s}}(t')$. Both of them will affect the bus injection (59).

While the first level of splitting is determined by the linear function (39), the second level of splitting is determined by the dispatch decision of each generator-storage pair, and is an undetermined function. The only thing that we know for the second level of splitting is that $\Phi_{\hat{s}^v_{g,s}}(t') \leq \overline{\Phi}_{\hat{s}^v_{g,s}}$. Thus, we seek to ensure that the transmission constraint (8) will hold for any demand splitting $D_{VGSP_{g,s}}(t')$ and $\Phi_{\hat{s}^v_{g,s}}(t') \leq \overline{\Phi}_{\hat{s}^v_{g,s}}$. Next, we first deal with all possible $\Phi_{\hat{s}^v_{g,s}}(t') \leq \overline{\Phi}_{\hat{s}^v_{g,s}}$.

Theorem 10. *One side of the transmission constraint $f_l(t') \leq TL_l$ holds if*

$$\sum_{b\in\mathcal{B}} S_{l,b}\big\{D_b(t') - \sum_{(g,s):g\in\mathcal{G}_b} D_{VGSP_{g,s}}(t')\big\} + \alpha_{g,s} \leq TL_l, \quad \text{for all } D(1:t)\in\mathcal{D}, \tag{61}$$

where $\alpha_{g,s} = \sum_{(g,s)} \left|S_{l,\mathcal{B}(g)} - S_{l,\mathcal{B}(s)}\right| \overline{\Phi}_{\hat{s}^v_{g,s}}$, and $\mathcal{B}(\cdot)$ returns the bus index where the generator or storage unit locates.

Proof. Using (59) and (60), the constraint $f_l(t') \leq TL_l$ can be written as

$$\begin{aligned}&\sum_{b=1}^{N_b} S_{l,b}\Big(D_b(t') - \sum_{g\in\mathcal{G}_b} P_g(t') - \sum_{s\in\mathcal{S}_b} \Phi_s(t')\Big) \\ &= \sum_{b=1}^{N_b} S_{l,b}\Big(D_b(t') - \sum_{(g,s):g\in\mathcal{G}_b} P_{\hat{g}^v_{g,s}}(t') - \sum_{(g,s):s\in\mathcal{S}_b} \Phi_{\hat{s}^v_{g,s}}(t')\Big) \\ &= \sum_{b=1}^{N_b} S_{l,b}\Big[D_b(t') - \sum_{(g,s):g\in\mathcal{G}_b} \Big(D_{VGSP_{g,s}}(t') - \Phi_{\hat{s}^v_{g,s}}(t')\Big) \\ &\qquad - \sum_{(g,s):s\in\mathcal{S}_b} \Phi_{\hat{s}^v_{g,s}}(t')\Big] \\ &= \sum_{b=1}^{N_b} S_{l,b}\Big(D_b(t') - \sum_{(g,s):g\in\mathcal{G}_b} D_{VGSP_{g,s}}(t')\Big) \\ &\qquad + \sum_{b\in\mathcal{B}} S_{l,b} \sum_{(g,s):g\in\mathcal{G}_b} \Phi_{\hat{s}^v_{g,s}}(t') - \sum_{b\in\mathcal{B}} S_{l,b} \sum_{(g,s):s\in\mathcal{S}_b} \Phi_{\hat{s}^v_{g,s}}(t') \\ &= \sum_{b=1}^{N_b} S_{l,b}\Big(D_b(t') - \sum_{(g,s):g\in\mathcal{G}_b} D_{VGSP_{g,s}}(t')\Big) \\ &\qquad + \sum_{(g,s)} \big[S_{l,\mathcal{B}(g)} - S_{l,\mathcal{B}(s)}\big]\Phi_{\hat{s}^v_{g,s}}(t') \qquad \leq \mathrm{TL}_l.\end{aligned} \tag{62}$$

Note that only the second summation term depends on $\Phi_{\hat{s}^v_{g,s}}$. Since $\Phi_{\hat{s}^v_{g,s}}(t') \leq \overline{\Phi}_{\hat{s}^v_{g,s}}$, it is sufficient if we can ensure that

$$\sum_{b=1}^{N_b} S_{l,b}\Big(D_b(t') - \sum_{(g,s):g\in\mathcal{G}_b} D_{VGSP_{g,s}}(t')\Big) + \sum_{(g,s)} \big|S_{l,\mathcal{B}(g)} - S_{l,\mathcal{B}(s)}\big|\overline{\Phi}_{\hat{s}^v_{g,s}} \leq TL_l,$$

which is exactly (61). Finally, (61) must hold for all $D(1:t) \in \mathcal{D}$. The result of the theorem then follows. □

Theorem 11. *The other side of the transmission constraint, i.e.,*

$$f_l(t') \geq -TL_l,$$

holds if

$$\sum_{b=1}^{N_b} S_{l,b}\Big(D_b(t') - \sum_{(g,s):g\in\mathcal{G}_b} D_{VGSP_{g,s}}(t')\Big) - \alpha_{g,s} \geq -TL_l, \quad \text{for all } D(1:t)\in\mathcal{D}, \quad (63)$$

where $\alpha_{g,s}$ and $\mathcal{B}(\cdot)$ are defined in the same way as in Theorem 10.

Proof. Theorem 11 can be shown in a similar way as Theorem 10. Hence, here the proof is omitted for concision. □

Then, we still need to check that (61) and (63) holds for all possible $D(t') \in \mathcal{D}_{t'|D(1:t)}$. We note that, for each $D(1:t)$, (61) and (63) are convex with respect to the virtualization and demand splitting parameters $A(t)$. Hence, the intersection over all $D(1:t)$ is also a convex constraint, although in a more complex form. To simplify, note that if there is only one uncertainty source in the system, i.e., $D(t') \in [D^{\min}(t'), D^{\max}(t')]$, the conditions can be verified by checking the extreme case when $D(t') = D^{\min}(t')$ or $D(t') = D^{\max}(t')$. If there are more than one renewable sources, the number of extreme cases become exponential in the number of renewable sources. Still, we can use a duality based approach in [8] to dualize the conditions in (61) and (63). This approach replaces each transmission constraint by a polynomial number of equivalent dualized constraints. See Section 4.1 in [8] for further details.

Appendix E
Convexification of Conditions in Theorem 7

The conditions in Theorem 7, i.e., equations (52) and (57), are not convex constraints. To see this, we can rewrite (52) as

$$Q_s^{\max} \geq \frac{\mathrm{Gap}(t)^2}{2(R_g-\beta)} - \frac{\mathrm{Gap}(t)^2}{2(\Delta-\beta)}. \quad (64)$$

Notice that each term on the RHS of the above equation is convex separately, as it is in a quadratic-over-linear form. However, the difference of two convex terms is usually not convex. Instead, we can use the following steps to obtain a sufficient condition to (52) that is convex. Note that

$$\frac{\mathrm{Gap}(t)^2}{2}\Big(\frac{1}{R_g-\beta} - \frac{1}{\Delta-\beta}\Big) = \frac{1}{2}\frac{\mathrm{Gap}(t)^2}{R_g-\beta}\frac{\Delta-R_g}{\Delta-\beta}.$$

Thus, (64) holds when

$$\Delta - R_g \leq \mathcal{C}(\Delta-\beta), \quad (65)$$

and

$$Q^{\max} \geq \frac{1}{2}\frac{\mathrm{Gap}(t)^2}{R_g-\beta}\mathcal{C}. \quad (66)$$

Note that by our formulation, $\Delta \geq R_g \geq \beta$. Thus, it implies that the constant $\mathcal{C}$ satisfies $\mathcal{C} \in [0,1]$. Now, the conditions (65) and (66) are convex constraints for any given constant $\mathcal{C}$. Then, we can iterate over $\mathcal{C}$ to improve the gap between (52) and its convex relaxation (65)-(66). The constraint (57) can be treated similarly.